Key Engineering Materials
ISSN: 1662-9795, Vol. 1051, pp 191-202
doi:10.4028/p-jx8Kt7

Submitted: 2026-01-19
Revised: 2026-02-24
Accepted: 2026-02-24
Online: 2026-04-17

Numerical-Experimental Study of Delamination in Crystalline Photovoltaic Panels to Support Efficient Recycling

Agata Sposato[1,a*], Giovanni De Martino[2,3,b], Gianni Stigliano[4,c], Claudio Cignali[4,d], Michele Dassisti[2,e], Domenico Umbrello[1,f]

[1]Department of Mechanical, Energy and Management Engineering, University of Calabria, Rende (CS) 87036, Italy

[2]Department of Mechanical, Mathematics and Management, Polytechnical University of Bari, Bari (BA) 70126, Italy

[3]Department of Sciences, Technologies and Society, University School of Pavia – IUSS Pavia, Pavia (PV) 27100, Italy

[4]KAD 3D S.r.l., Monopoli (BA) 70043, Italy

[a*]agata.sposato@unical.it, [b]giovanni.demartino@poliba.it, [c]stigliano@kad3.com, [d]cignali@kad3.com, [e]michele.dassisti@poliba.it, [f]domenico.umbrello@unical.it

Keywords: photovoltaic panels, cryogenic delamination, finite element modelling, material characterisation.

Abstract. In the global transition towards renewable energy, a leading role is played by photovoltaic (PV) technologies. However, the increasing growth of installed PV panels, together with the rise of the number of modules reaching their end-of-life phase, make the sustainable management of electronic waste a crucial aspect. The reduction of energy consumption and polluting emissions and the maximization of material recovery represent the ultimate purpose of demanufacturing processes. Here, cryogenic delamination is proposed as an innovative strategy, as it exploits the thermal and mechanical properties of PV module constituents to achieve the cleanest possible separation of layers, allowing for the recovery of strategic materials (silicon, aluminium, silver, copper). This work aims to combine experimental and numerical approaches in order to obtain a comprehensive understanding of the fundamental mechanisms governing the process: the overall objective is represented by the process optimization to enable the exploration of various operating conditions without the need for costly and time-intensive experimental campaigns and, ultimately, the implementation of such technology at the industrial scale.

Introduction

Photovoltaic cells are the functional unit of a photovoltaic panel (PVP); typically manufactured from monocrystalline or polycrystalline silicon, they enable the conversion of light into electrical energy [1]. PV cells are incorporated into the PVP multilayer by two polymer layers: the first layer works as an adhesive, bonding the silicon cells to the glass substrate; the second one protects the cells against adverse environmental conditions [2, 3]. The four layers are placed onto a backsheet and mechanically supported by a surrounding frame (Fig. 1) [4].

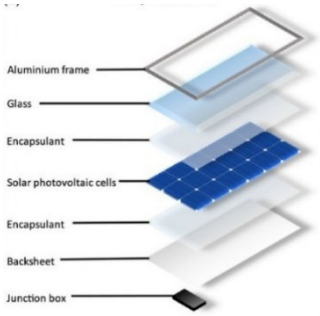

Fig. 1. Layered structure of a crystalline silicon PV module. [2].

A hot lamination process ensures the bonding of the various layers, as complete adhesion between materials and effective insulation from external agents are reached [5]. However, given its irreversible nature, it considerably hinders PVPs disposal at the end of their service life: thus, issues in separating the constituent materials often lead to panels being discarded in landfill sites [6].

In view of the continuous growth in installed PV capacity and the increasing number of panels entering their end-of-life phase, the sustainable management of PV waste represents a crucial aspect. The generation of waste from PV modules is directly associated with their average operational lifetime, which is estimated to range between 20 and 30 years [7]; given global PV installations peaked between 2010 and 2020, a doubling of photovoltaic waste volumes is expected by 2035. As a result, the sustainability of dismantling processes must focus on reducing energy consumption, minimising polluting emissions, and maximising the efficient recovery of constituent components [8]. From this perspective, demanufacturing techniques represent a more targeted and strategic approach to manage electronic and industrial waste, as they enable the separation of recyclable materials and the recovery of components that remain functional or repairable [9]. In this way, it is possible to not only mitigate the environmental impact by reducing the amount of waste destined to landfill disposal or incineration, but also to enhance the recovery of valuable resources while fostering new economic opportunities centred on recycling and material reuse.

Existing demanufacturing methods can generally be categorised as physical, thermal or chemical treatments, listed in order of increasing quality of recovered components, as well as rising levels of complexity and cost [10, 11]. However, despite the wide range of approaches proposed in the literature, an optimal demanufacturing process has yet to be identified. The main limitation of technologies employed to date lies in the fact that, whether destructive or semi-destructive (only the connecting elements are destroyed), such methods tend to substantially alter the physical and chemical properties of the processed materials, often making them unsuitable for applications requiring high technological performance [12].

A promising strategy involves the application of thermo-mechanical treatments to induce delamination, intended as the progressive weakening and eventual rupture of the interfacial bonds between adjacent layers, leading to their separation [13]. The demanufacturing approach proposed here, known as cryogenic delamination, exploits the distinct thermal and mechanical properties of the materials constituting a PV panel in order to achieve the cleanest separation of its components [14].

The purpose of the present study is to conduct in parallel experimental tests and a numerical modelling study within a finite element analysis (FEA) framework in order to obtain a comprehensive understanding of the mechanisms governing the cryogenic delamination process. The objective is to calibrate the model against experimental evidence collected in the laboratory so that the two aspects are constantly interconnected and the physics of the problem are never lost sight of. The research thus performs a comparative numerical and experimental investigation in order to develop and validate a FE model capable of accurately reproducing the actual behaviour of the system. A high level of correspondence allows for both the optimisation of the procedure and the assessment of its potential scalability for continuous industrial application. Once validated through comparison with experimental data – particularly with regard to temperature evolution, as well as the stresses and displacements generated –, the FE model allows for the exploration of different process conditions without the need for costly and time-consuming experimental campaigns [15, 16].

It is important to point out that this work represents the first step in a broader study aimed at optimising the cryogenic delamination process to enable the implementation of the technology at an industrial level. For this reason, the following discussion is purely phenomenological in nature and focuses on the study of thermal aspects for a quantitative and in-depth analysis; on the other hand, at present, mechanical analyses are limited to an exploratory and therefore qualitative state. Future studies will aim to investigate the correspondence between the actual behaviour of the delaminated photovoltaic module and the behaviour predicted by the numerical analysis, in order to validate the models chosen to represent the elastoplastic behaviour of the various materials and their damage evolution up to failure.

Theoretical Bases of the Cryogenic Delamination Process

In PV modules, materials with significantly different thermal behaviours must coexist while preserving structural integrity throughout their operational lifespan. The inorganic constituents – namely crystalline silicon and annealed soda-lime silicate glass – exhibit relatively low and comparable coefficients of thermal expansion (CTE) [17]; by contrast, ethylene-vinyl acetate (EVA), which is the most commonly employed encapsulant, displays a CTE almost two orders of magnitude higher [18].

Within the operational temperature range, the encapsulant experiences both glass transition and melting phenomena [22], making its thermal response a critical factor for long-term module durability. The mechanical properties of the material change abruptly across the glass transition temperature (T_g) [23]: below this threshold, the polymer is stiff and brittle, whereas above it, it exhibits a viscoelastic and compliant behaviour. This transition has a decisive influence on the mechanical integrity of the cell-encapsulant interface. Consequently, close attention must be paid to both the value of T_g and the evolution of the storage modulus, which stabilises at approximately −40°C following crosslinking [24] – a temperature commonly identified as the lower limit for reliable module operation. A thorough understanding of this embrittlement mechanism is therefore essential for predicting thermomechanical fracture at module interfaces.

The relevant values of thermal expansion coefficients and glass transition temperatures for the principal materials used in PV modules are reported in Table 1.

Table 1. Thermomechanical properties of PV module materials.

Material	Type of material	CTE [K^{-1}]	T_g [°C]
Crystalline silicon (c-Si)	Inorganic semiconductor	2.6×10^{-6} [17]	–
Soda-lime silicate glass (annealed)	Inorganic glass	9×10^{-6} [19]	–
EVA (encapsulant)	Polymeric encapsulant	$1.6 \times 10^{-4} – 2.5 \times 10^{-4}$ [18]	-36 (pre-/post-lamination) [20] -33.1 (PV-grade EVA) [21] -16.9 (after crosslinking) [22]

In multi-material systems exposed to cyclic thermal variations, interfacial stresses arise as a direct consequence of mismatches in CTE [21]. In the case of PV panels, in response to thermal variations the polymer undergoes expansion and contraction to a far greater extent than the surrounding crystalline materials. Thus, stress accumulation at the glass-encapsulant and cell-encapsulant interfaces frequently act as initiation sites for microcracks along mechanically fragile crystallographic planes within the silicon layer during both manufacturing-related thermal treatments and in-service thermal cycling, particularly when operating temperatures approach or exceed the polymer glass transition temperature.

This temperature-dependent degradation mechanism occurring at the glass-EVA-silicon interfaces represents the conceptual foundation of cryogenic delamination, which deliberately exploits the pronounced contrast in thermal behaviour between the crystalline layers and the EVA encapsulant. By imposing controlled thermal excursions, the process selectively weakens interfacial adhesion and promotes crack propagation through the encapsulant, ultimately resulting in interfacial failure, while preserving the structural integrity of high-value materials. The thermo-mechanical procedure has been formalised in patent [25]. By applying thermal gradients, tangential stresses are generated at the interfaces; by inducing selective failure within the polymeric interlayers while maintaining the integrity of the rigid components, the process enables effective layer separation without the need for aggressive chemical treatments or high-temperature pyrolysis, thereby preserving the quality and potential reusability of the recovered silicon and glass substrates.

Materials and Methods

Testing methods.

The experimental campaign was carried out on specimens extracted from end-of-life crystalline silicon photovoltaic modules, encompassing both mono- and polycrystalline technologies to ensure the industrial relevance and practical applicability of the results to large-scale recycling processes, as these constitute the predominant categories of the current photovoltaic panel waste. The representative modules stratigraphy (Table 2) comprises: a front layer of low-iron soda-lime glass; a first encapsulating EVA layer; crystalline silicon solar cells featuring metallisation grids, typically consisting of silver busbars and aluminium back contacts; a second EVA layer; a polymeric backsheet, typically made of polyvinyl fluoride (Tedlar). The backsheet will not be considered for the following analyses, as its behaviour does not influence the delamination phenomena.

Table 2. Stratigraphy of the considered photovoltaic modules.

Material	Thickness [mm]
Glass	3.2
EVA	0.4
Silicon	0.2
EVA	0.4

Specimens were prepared using water-jet cutting technology to preserve the structural integrity of the laminated assembly and minimise the likelihood of introducing microcracks or other artefacts prior to testing. Each sample was individually weighed and systematically catalogued to ensure full traceability and to allow a rigorous mass balance analysis throughout the delamination procedure. The sample dimensions were standardised to 160×160 mm² to limit variability in thermal response; however, a certain level of dimensional heterogeneity was tolerated, owing to constraints associated with the availability of decommissioned photovoltaic modules.

Experimental set-up.

The experimental apparatus exploited a cryogenic system employing a pressurised liquid nitrogen (LN_2) jet: this arrangement enabled accurate control over both the magnitude and the localisation of the thermal shock to be imposed, in accordance with the principles described in the patent [25]. To this end, a cryogenic Dewar vessel was connected to a pressure regulation unit equipped with an on–off valve, which allowed modulation of the LN_2 jet delivered to the target surface of the photovoltaic sample. Different operating pressures were investigated, in order to optimise the thermal gradient and the effectiveness of the delamination process. The selected operating pressure was 9 bar, representing a balance between jet momentum, liquid nitrogen consumption and safety constraints; under these conditions, the LN_2 jet produced a rapid and localised temperature decrease on the rear surface of the module, thereby inducing the required thermomechanical stresses across the laminate thickness. The most relevant parameters governing the delamination process are summarised in Table 3.

Table 3. Operating parameters of the cryogenic delamination setup.

Parameter	Specification	Parameter	Specification
Cryogenic medium	Liquid nitrogen (LN_2) jet	Heating system	Two hot air guns
Supply system	Dewar vessel with pressure regulation	Heating temperature	≈ 300 °C
Operating pressure	9 bar	Thermal strategy	Front heating + rear cryogenic cooling
Cooling target	Rear surface of PV module	Aspiration system	Vapor extraction near sample holder

The experimental procedure followed a standardised sequence of steps to induce the differential thermal shock mechanism underlying the cryogenic delamination.

- Front surface heating. The photovoltaic sample was mounted vertically within the test rig and heated by two industrial hot-air guns directed towards the glass surface until a surface temperature of approximately 300°C was reached, as measured using an infrared thermometer. This phase typically lasted a few minutes, depending on ambient conditions and sample thermal mass.
- Cryogenic jet application. The pressurised LN_2 jet was directed onto the rear surface of the sample (corresponding to the backsheet side). An operating pressure of 9 bar ensured a high-velocity jet capable of rapidly extracting heat from the rear layers of the laminate. The cryogenic jet was applied for approximately 1 min per sample, a duration determined empirically to induce a significant thermal shock while limiting nitrogen consumption.
- Post-treatment observation. When the sample reached thermal equilibrium, visual and tactile inspections were carried out to evaluate the extent of delamination, the presence of cracks and the integrity of the individual layers.

The combined action of front-side heating and rear-side cryogenic cooling generated the differential expansion and contraction stresses responsible for interfacial failure within the adhesive layers. The apparatus incorporated an aspiration system to manage the nitrogen vapour produced during LN_2 evaporation; this system fulfilled both safety and operational roles, ensuring adequate ventilation of the working environment and limiting the formation of condensation and frost on adjacent equipment.

Numerical modelling.

Finite element (FE) simulations applied to PV modules cryogenic delamination represent a powerful computational tool to estimate the temperature evolution, the distribution of interfacial stresses and the damage mode and paths during thermal cycling processes. The FE software employed for the analyses was DEFORM, developed and distributed by Scientific Forming Technologies Corporation (SFTC).

Material characterisation.

To represent the effects of the applied thermal load – being the only external loading condition – in terms of both temperature variations and stress and deformations fields induced within the multilayer assembly, both thermal and mechanical aspects were included in the analysis. The multilayer system was modelled to replicate the PV module employed for the experimental tests, specifically a 160×160 mm² square specimen (Fig. 2a). The thickness of each layer was established on the basis of the stratigraphy reported in Table 3; given the geometric regularity of the system, a brick-type mesh was adopted. The number of elements assigned to each component was selected to ensure full nodal compatibility at the interfaces (Fig. 2b).

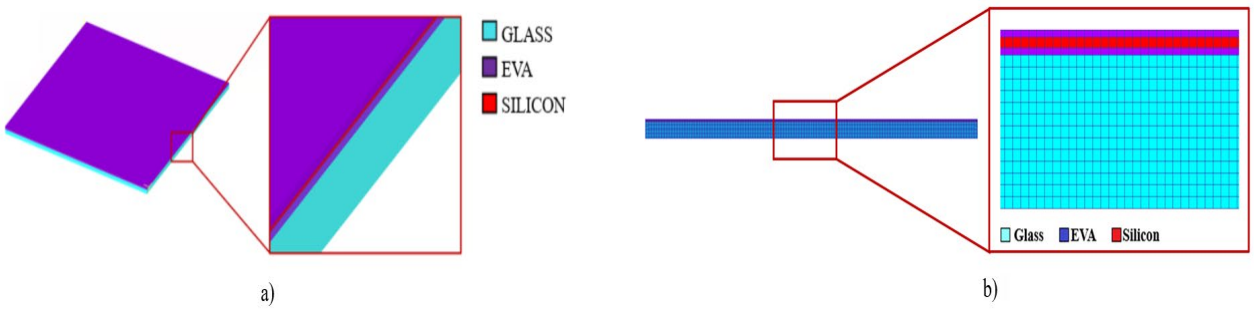

Fig. 2. a) 3D model of the PV module. b) 2D meshed multilayer module.

The material properties attributed to each layer were obtained from the relevant scientific literature; the principal thermo-mechanical parameters are summarised in Table 4. For the purposes of numerical analysis, the properties assigned to the encapsulant layers refer to a homogeneous and

non-aged material. These are, of course, simplifications: in fact, not only do polymers, by virtue of their molecular composition, not have homogeneous characteristics, but also real end-of-life PV modules have necessarily undergone ageing and therefore experienced a degradation of their initial characteristics due to the thermal cycles and the action of atmospheric agents to which they were constantly subjected.

Table 4. Thermomechanical properties of PV module materials for simulation purposes [17-22].

Material	Thermal conductivity [W/mK]	Specific heat [J/kgK]	Emissivity [-]	Young's modulus [MPa]	Poisson's coefficient [-]
Glass	1	800	0.9	70	0.65
EVA	0.25	2300	0.9	0.65	0.43
Silicon	150	700	0.65	160	0.28

A key aspect concerned the definition of the constitutive equations governing the plastic flow behaviour of the materials involved (Table 5).

At 300°C (cryogenic delamination process starting temperature), EVA does not behave like a normal polymer in melt, as it undergoes rapid thermal degradation: in fact, its typical processing temperature is usually below 200°C, while deacetylation begins at 290°C-300°C, with the formation of double bonds and polyenes. However, when analysed over a very short time window, the plastic flow law of molten EVA follows the pseudoplastic fluid (power-law fluid) model, characterized by shear thinning, with main parameters: τ shear stress; $\dot{\gamma}$ shear rate; n flow behaviour index (less than 1 for pseudoplastic polymers); K consistency index (viscosity).

From a molecular point of view, glass is an amorphous solid (or at least comparable to a supercooled liquid with extremely high viscosity). Unlike crystalline materials, glass has a disordered and disorganized structure. At 300°C, since it is still below its glass transition temperature (usually T_g>500°C), glass behaves like a linear elastic or viscoelastic solid rather than a viscous fluid in plastic flow. Its behaviour is therefore described by Hooke's law, whereby the stress state developed within the material depends on its stiffness (expressed in terms of Young's modulus E) and the deformation achieved ε.

At 300°C, which corresponds to about one third of its melting point, crystalline silicon is in a brittle-ductile transition regime, and its plastic deformation is mainly governed by the movement of dislocations (in particular by the overcoming of Peierls barriers): these are partial dislocations that form microtwins and stacking faults; however, the movement of the dislocation segments is still quite limited. Silicon plastic behaviour is therefore governed by an exponential or power law (Arrhenius-type law), typical of crystalline viscoplasticity and similar to that of low-temperature creep, where the plastic deformation rate ($\dot{\gamma}^p$) is proportional to a power of the resolved stress (τ). τ_c is the Critical Resolved Shear Stress (CRSS); n is the strain-rate sensitivity exponent.

Table 5. Flow stress laws of PV module materials.

Material	EVA	GLASS	Silicon
Flow Stress law	$\tau = K \cdot \dot{\gamma}^n$	$\sigma = E\varepsilon$	$\dot{\gamma}^p = \dot{\gamma}_0 \left\lvert \frac{\tau}{\tau_c} \right\rvert^n$

Boundary and loading conditions.

The boundary conditions were defined to reproduce the experimental setup configuration, where the photovoltaic module is clamped along a portion of its perimeter to constrain displacements in all spatial directions within the clamped region (Fig. 3).

Fig. 3. a) Clamp used for the experimental tests; b) modelled boundary condition.

In terms of thermal interactions, natural (i.e. non-forced) heat exchange was prescribed between all external surfaces of the PV multilayer and the surrounding environment, which was assumed to be at a uniform temperature of 20°C. The external heating device was represented as an industrial heat gun characterised by a nominal power of 1.8 kW, three temperature settings (50/300/600°C), and three airflow rates (200/350/500 $l \cdot min^{-1}$). The convective heat flux was evaluated using the fundamental thermodynamic relation (Eq. 1):

$$Q = hA(T_f - T_p) \tag{1}$$

where: Q is the heat flux [W]; h is the convective heat transfer coefficient [$W/(m^2 \cdot K)$]; A is the heat exchange area [m^2]; T_f is the temperature of the fluid (hot air) [°C]; T_p is the temperature of the wall (i.e. the colder surface) [°C]. Since h depends on parameters such as type of convection, surface geometry, and fluid properties, an average representative coefficient of 225 $W/(m^2 \cdot K)$ was adopted, consistent with forced convection under high-velocity turbulent flow conditions. The heat gun was considered to operate at its maximum temperature (T_f=600°C). As the heat source is positioned at an approximate distance of 10 cm from the glass surface and therefore a temporal delay precedes the onset of significant heating, a time-dependent ramp-shaped heat flux was implemented and calibrated against experimental measurements.

Regarding the cryogenic fluid application, while experimentally LN_2 was delivered via a nozzle, for modelling purposes the entire upper EVA surface was subjected to its action, corresponding to a thermal boundary condition of T = −182 °C with the associated convective heat transfer coefficient defined as a time-dependent function according to the Astakhov–Joksch model (Eq. 2):

$$h_{cryo} = \frac{0.20}{e^{0.35} g^{0.33}} \frac{V_f^{0.65} k_f^{0.67} c_p^{0.33} \gamma_f^{0.33}}{\nu_f^{0.32}} \tag{2}$$

Interfacial bonding conditions.

The interactions between adjacent layers were defined through interfacial bonding conditions influencing both heat transfer and mechanical behaviour, including the development of residual stresses. For each interface (Glass-EVA1, EVA1-Silicon, Silicon-EVA2), a conductive heat transfer coefficient was calculated according to Eq. 3:

$$\frac{1}{U_{Cond}} = \sum \frac{S_n}{k_n} \tag{3}$$

where U_{cond} defines the overall conductive heat transfer coefficient [$W/(m^2 \cdot K)$], S_n is the thickness of the n-th layer [m], and k_n represents the thermal conductivity of the n-th layer [$W \cdot m^{-1} \cdot K^{-1}$].

In addition, the Sticking Condition option was enabled to model a complete and perfect adhesion at each interface between layers, thereby reproducing the bonding effect provided by the polymer encapsulant. To model delamination triggered by cryogenic loading, a non-geometric separation criterion was subsequently implemented: more specifically, interfacial separation was allowed once a prescribed fraction of the material flow stress was attained. This threshold value was calibrated through a combination of preliminary numerical simulations performed without delamination and experimental evidence, which indicated the onset of detachment after approximately 5s from the beginning of the process. However, in this initial investigation, no fracture or damage criteria were

implemented for the finite elements within the FE software, thereby preventing an accurate prediction and description of material cracking phenomena.

The numerical analysis was performed over a total duration of 100s, discretised into 500 time steps, so as to ensure a detailed representation of the thermo-mechanical evolution of the system.

Results and Discussion

In laboratory tests, the observed delamination patterns proved to be markedly complex: the cryogenically treated samples displayed pronounced structural degradation of the laminate, involving internal cracking, polymer fragmentation, and irregular weakening and failure at the glass-EVA and EVA-silicon interfaces. This heterogeneous response can be ascribed to variations in module ageing, encapsulant compositions, and thermal histories across the end-of-life panels examined (Fig. 4).

More specifically, internal cracking of the silicon solar cells was consistently observed during cryogenic exposure; this phenomenon was attributed to the combined action of thermal shock and the inherent brittleness of crystalline silicon at extremely low temperatures. Such fragmentation enhances the mechanical release of silicon particles from the surrounding polymer matrix, thereby facilitating subsequent material recovery processes; conversely, cell fracture also constitutes a limitation, as it precludes the retrieval of intact silicon wafers suitable for direct reuse.

The EVA encapsulant layers were only partially and discontinuously removed, with substantial residual adhesion persisting on both the glass and silicon surfaces. Instead of separating as continuous films, the polymer predominantly failed cohesively, leaving fragments attached to both substrates. This partial separation suggests that controlled cryogenic shock effectively degrades interfacial bonding and induces mechanical stresses within the polymer matrix, yet remains insufficient to achieve complete material liberation in a single processing step.

Fig. 4. Post-treatment PV laminate samples.

On the other hand, the numerical results indicated a clear detachment of the EVA surface layer in the portion of the PV module not constrained by the clamp, whereas separation of the silicon cell substrate from the lower encapsulant layer appeared significantly more limited (Fig. 5) This result, which is essentially phenomenological in nature, is confirmed by experimental observations in terms of the extent of the delaminated area, since in the time interval considered (5s) the delamination involves only a small portion of the material. Obviously, as the exposure time of the photovoltaic module increases and consistently with a variation of the temperature reached inside the multilayer, the area undergoing delamination changes accordingly.

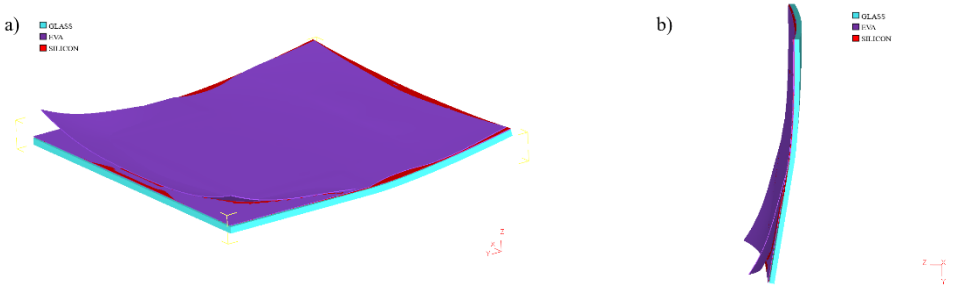

Fig. 5. FE predicted delamination: a) on isometric view; b) on lateral view.

Notwithstanding this agreement, a substantial divergence was identified between the numerical outcomes and the experimental evidence, as the former showed an idealised layer-by-layer separation exhibiting clean interfacial failure at the glass-EVA and EVA-silicon interfaces. The mismatch between the neat delamination predicted numerically and the incomplete, heterogeneous separation observed experimentally can be attributed to the preliminary nature of the FE model. As specified among the assumptions made in order to simplify the modelling in such an initial investigation phase, no fracture criteria were implemented: the absence of specific material models aimed at defining the damage progression and the cracking mode for the finite elements necessarily prevents an accurate description of material breaking phenomena, representing each element as deformable but not subject to internal disruption. The introduction of appropriate fracture criteria would obviously enable the prediction of the location and onset of material failure as a function of the stress and strain states attained during processing, together with material-specific damage parameters. Accordingly, future developments of the model will concentrate on integrating a dedicated fracture subroutine informed by recent literature: such an improvement is expected to narrow the gap between simulation and experimental observations, ultimately providing a robust predictive tool for the analysis of PV module delamination under diverse thermal and mechanical conditions. The availability of such a model would also reduce reliance on costly and time-consuming experimental campaigns.

As stated before, thermal aspects were evaluated quantitatively for validation purposes: surface temperature was therefore adopted as the main variable for evaluating the boundary conditions governing heat exchange with the environment. Experimentally, the LN_2 jet was applied once the external glass surface reached a uniform temperature of 300°C. In the simulation, the corresponding temperature at this stage was 293°C, resulting in a percentage deviation of 2.3%, which can be considered negligible (Fig. 7a). After cryogenic treatment, the predicted glass surface temperature decreased to 258°C, compared with an experimentally measured value of 260°C; the associated error of 0.4% further corroborates the satisfactory thermal accuracy of the model (Fig. 7b).

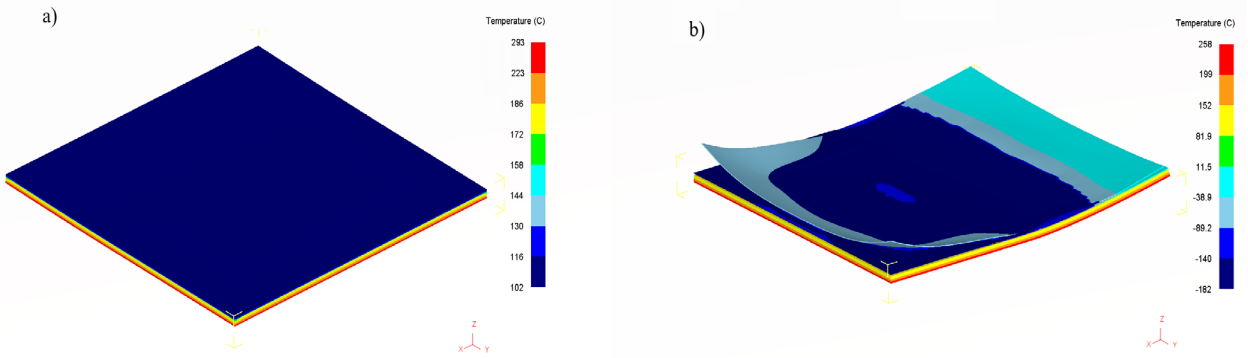

Fig. 6. Temperature distribution: a) before the cryogenic treatment; b) after the cryogenic treatment.

At the current stage, assessment of the plastic behaviour of the materials through direct comparison between numerical results and experimental data was not feasible, as no instrumentation was employed to monitor stress states within the multilayer assembly. Consequently, it cannot yet be ascertained whether the implemented plastic flow laws can capture the actual stress-strain behaviour. Looking ahead, given the internal nature of the defects, Non-Destructive Techniques (NDT) based on integrated sensors are expected to be used to measure stress levels and monitor the progression of deformations during delamination. In terms of stress, since techniques capable of detecting both residual (generated during production) and operating stresses – often concentrated in interface areas – are required, Acoustic Emission (AE) stands out as it allows delamination to be monitored in real time: in fact, piezoelectric sensors detect the transient elastic waves generated by the sudden release of energy during matrix cracking or layer separation. On the other hand, concerning the assessment of deformations, Digital Image Correlation (DIC), as a non-contact optical technique, enables the measurement of displacement and surface deformation fields and thus the identification of areas of high deformation associated with the opening of the delamination crack.

Conclusion

Cryogenic delamination was presented here as an innovative as well as environment- and energy-friendly demanufacturing strategy for end-of-life PV panels, capable of enabling the separation of the materials composing the multilayer structure by exploiting their differences in thermal and mechanical characteristics.

From an experimental perspective, post-treatment analysis revealed a partial separation of the constituent materials, with substantial residual polymer adhesion on both glass and silicon surfaces. The experimental evidence thus confirms that cryogenic delamination functions effectively as a mechanical pre-treatment, as it weakens interfacial bonding and induces fragmentation within the multilayer assembly; however, it is not sufficient, on its own, to achieve complete material separation. These outcomes have led to the formulation of a two-stage recycling strategy – currently under development – where cryogenic thermal shock, representing the first operating stage, is subsequently complemented by a chemical treatment intended to accomplish total material separation and surface cleaning. This second phase is designed and expected to remove polymer residues through the application of mild chemical agents under controlled conditions, thereby minimising environmental impact. The sequential coupling of mechanical and chemical processes is anticipated to exploit the strengths of both approaches while alleviating their respective shortcomings.

In terms of numerical modelling, the study focused on phenomenological and thermal aspects for a quantitative analysis. The calibration of the FE model against laboratory experiments revealed a good agreement in terms of surface temperature evolution, thus revealing an accurate modelling of the thermal aspects of the materials involved. On the other hand, mechanical analyses had an exploratory and qualitative nature, given the limits exhibited both in the measuring systems for stress and strain evolution and in the definition of criteria for reproducing the damage progression and final cracking of materials involved in the FE environment. Forthcoming efforts will therefore concentrate on validating of the simulated plastic behaviour through a dedicated experimental programme aimed at monitoring the stress states and the deformation progression developing within the multilayer structure, as they are responsible for material detachment. In parallel, integrating an appropriate fracture criteria in order to reproduce the material fragmentation induced by the hot-cold thermal shock sequence will be pursued.

The ultimate purpose of this research is to develop a robust predictive model capable of faithfully representing delamination phenomena under well-defined operational conditions, making it possible to facilitate the industrial-scale implementation of the proposed process.

Acknowledgement

This work was supported by the European Union - NextGenerationEU, under the Italian National Recovery and Resilience Plan (PNRR), Mission 4 Component 2 Investment 1.3 - Partenariato Esteso NEST (Network 4 Energy Sustainable Transition) - project code PE000021.

Sections “2. Theoretical bases of the cryogenic delamination process” “3.1. Testing methods” were produced while attending the PhD programme in Sustainable Development and Climate Change at the University School for Advanced Studies IUSS Pavia, Cycle XXXIX, with the support of a scholarship financed by the Ministerial Decree no. 118 of 2023, based on the NRRP - funded by the European Union - NextGenerationEU - Mission 4 "Education and Research", Component 1 "Enhancement of the offer of educational services: from nurseries to universities" – Investment 4.1 “Extension of the number of research doctorates and innovative doctorates for public administration and cultural heritage”.

This work was supported by the Italian Ministry of Education, University and Research under the Programme “Department of Excellence” 2018-2022 and 2023-2027 – Italian Law 232/2016 (Grant No. CUP - D94I18000260001).

References

[1] M. Aghaei, A. Fairbrother, A. Gok, S. Ahmad, S. Kazim, K. Lobato, et al., Review of degradation and failure phenomena in photovoltaic modules, Renew. Sustain. Energy Rev. 159 (2022) 112160.

[2] J. Lee, N. Duffy, J. Allen, A review of end-of-life silicon solar photovoltaic modules and the potential for electrochemical recycling, Adv. Energy Sustain. Res. 6 (2025).

[3] N.Tz. Dintcheva, E. Morici, C. Colletti, Encapsulant materials and their adoption in photovoltaic modules: a brief review, Sustainability 15 (2023) 9453.

[4] G. Wei, Y. Zhou, Z. Hou, Y. Li, Q. Liu, J. Chen, et al., Review of c-Si PV module recycling and industrial feasibility, EES Solar 1 (2025) 9–29.

[5] Advances in photovoltaic module recycling literature review and update to empirical life cycle inventory data and patent review, Task 12 PV Sustainability Activities (n.d.).

[6] S. Xia, Y. Yang, J.P.H. Poon, How to tackle the looming challenge of solar PV panel recycling, Proc. Natl. Acad. Sci. U.S.A. 122 (2025).

[7] T. Dimitriou, N. Skandalos, D. Karamanis, Progress in improving photovoltaics longevity, Appl. Sci. 14 (2024) 10373.

[8] S. Kwon, H.J. Kim, S. Kim, S.J. Hong, Sustainability impact evaluation of the recycling of end-of-life crystalline silicon solar photovoltaic panel waste in South Korea, Sustainability 17 (2025) 431.

[9] F. Borda, R. Adduci, D. Mundo, F. Gagliardi, Cumulative energy demand analysis of commercial and hybrid metal-composite gears at different end-of-life strategies, J. Manuf. Mater. Process. 9 (2025) 14.

[10] M. Martínez, Y. Barrueto, Y.P. Jimenez, D. Vega-Garcia, I. Jamett, Technological advancement in solar photovoltaic recycling: a review, Minerals 14 (2024) 638.

[11] B. Al Zaabi, A. Ghosh, Managing photovoltaic waste: sustainable solutions and global challenges, Sol. Energy 283 (2024) 112985.

[12] G. Serratore, F. Borda, V. Basile, L. Filice, Life cycle assessment-guided design for sustainable microinjection molds, in: Proc. …, (2025) 1807–1816.

[13] D. Wu, P. Wessel, J. Zhu, D. Montiel-Chicharro, T.R. Betts, A. Mordvinkin, et al., Influence of lamination conditions of EVA encapsulation on photovoltaic module durability, Materials 16 (2023).

[14] A. Surowiak, M. Wahman, Thermal–mechanical delamination for recovery of tempered glass from photovoltaic panels, Energies 17 (2024) 4444.

[15] O. Hasan, A.F.M. Arif, M.U. Siddiqui, Finite element modeling, analysis, and life prediction of photovoltaic modules, J. Sol. Energy Eng. 136 (2014).

[16] G. Serratore, F. Borda, A.M. Igor Cosma, F. Gagliardi, L. Filice, A digital twin architecture for monitoring and quality assessment for a composite filament extrusion pilot line, Procedia Comput. Sci. 253 (2025) 3133–3142.

[17] S. Rollo, D. Rani, W. Olthuis, C. Pascual García, Single step fabrication of silicon resistors on SOI substrate used as thermistors, Sci. Rep. 9 (2019) 2835.

[18] J. Jackson, A. Chen, H. Zhang, H. Burt, M. Chiao, Design and near-infrared actuation of a gold nanorod–polymer microelectromechanical device for on-demand drug delivery, Micromachines 9 (2018) 28.

[19] V.-A. Silvestru, R. Giesecke, B. Dillenburger, Structural behaviour and micro-structural characteristics of coloured kilned glass panels, Glass Struct. Eng. (2022).

[20] M. Baiamonte, C. Colletti, A. Ragonesi, C. Gerardi, N.Tz. Dintcheva, Durability and performance of encapsulant films for bifacial heterojunction photovoltaic modules, Polymers 14 (2022) 1052.

[21] P.F.C. Videira, R.A. Ferreira, P. Maleki, A. Akhavan-Safar, R.J.C. Carbas, E.A.S. Marques, et al., Impact of thermal variations on the fatigue and fracture of bi-material interfaces found in microchips, Polymers 17 (2025) 520.

[22] R. Polanský, M. Pinkerová, M. Bartůňková, P. Prosr, Mechanical behavior and thermal stability of EVA encapsulant material used in photovoltaic modules, J. Electr. Eng. 64 (2013) 361–365.

[23] P. Kartikay, K. Mokurala, B. Sharma, R. Kali, N. Mukurala, D. Mishra, et al., Recent advances and challenges in solar photovoltaic and energy storage materials: future directions in Indian perspective, J. Phys. Energy 3 (2021) 034018.

[24] M. Dassisti, G. Florio, F. Maddalena, Cryogenic delamination and sustainability: analysis of an innovative recycling process for photovoltaic crystalline modules, in: Sustain. Des. Manuf. (2017) 637–646.

[25] M. Dassisti, Thermo-mechanical controlled cryogenic delamination process for the full recovery of rigid mono-, polycrystalline or amorphous materials coated with plastic materials, WO 2014/141311 A1 (2014).